Electronic Supplementary Material (ESI) for Environmental Science: Nano.

Supporting Information

Selective catalytic oxidation of ammonia over nano Cu/zeolites of different topologies

Hao Wang,[1] Runduo Zhang,[1,*] Yiyun Liu,[2] Peixin Li,[1] Hongxia Chen,[1] Feng Ryan Wang,[2] Wey Yang Teoh[3,*]

[1]State Key Laboratory of Chemical Resource Engineering, Beijing Key Laboratory of Energy Environmental Catalysis, Beijing University of Chemical Technology, 100029 P. R. China

[2]Department of Chemical Engineering, University College London, Torrington Place, London WC1E 7JE, United Kingdom

[3]School of Chemical Engineering, The University of New South Wales, Sydney, NSW 2052, Australia

*Corresponding author: R. Zhang (zhangrd@mail.buct.edu.cn);

W. Y. Teoh (wy.teoh@unsw.edu.au)

Catalyst Preparation

Nanoparticle ZSM-5 zeolite was synthesized by a hydrothermal method, the molar ratio of the mixture composition was 100 SiO_2 : $2Al_2O_3$: $2Na_2O$: 26.9 TPA^+ : 3700 H_2O. After stirring at 35 ^oC for 4 h, the solution was then heated at 80 ^oC to remove ethanol produced during the hydrolysis of TEOS, and water was added to maintain a constant volume. After crystallization at 170 ^oC for 3 days, the powder was recovered by centrifugation and dried at 100 ^oC for 12 h. Finally, the powder was calcined in air at 550 ^oC for 8 h to remove the organic template. The zeolites synthesized in the laboratory were generally of Na-form. They were ion-exchanged with 1 M NH_4NO_3 (50 ml/g zeolite) solution at 80 ^oC under stirring for 6 h, and this process was repeated 3 times to convert the Na-form zeolites into NH_4-form zeolites. After drying for 8 h, the samples were calcined at 550 ^oC for 5 h to obtain H-form zeolites.

Mn and Fe/ZSM-5 catalysts with wt.3% metal loadings were synthesized by impregnation in an analogous procedure as the Cu/ZSM-5 as described in the Experimental Section. Likewise, the noble metal Ag, Pd and Pt/ZSM-5 were also prepared by the analogous impregnation procedure but with final metal loading of 0.5 wt.%.

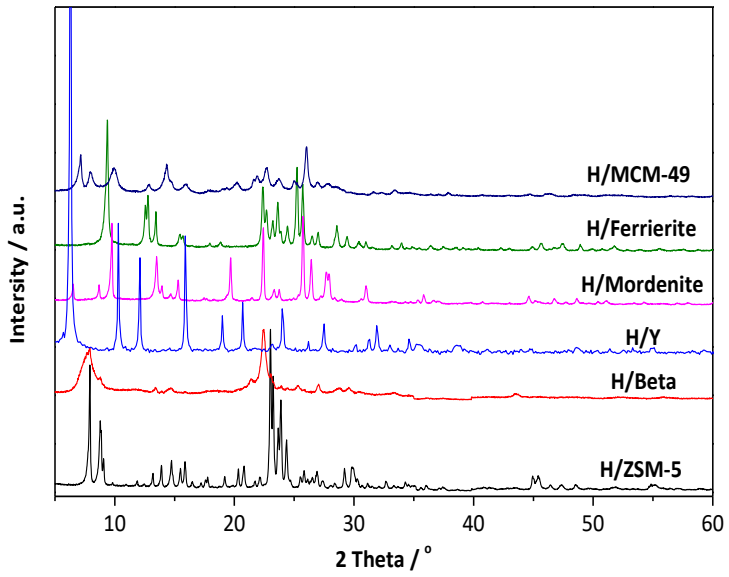

Fig. S1. XRD patterns of pristine H/zeolites (ZSM-5, Beta, Y, Mordenite, Ferrierite, and MCM-49).

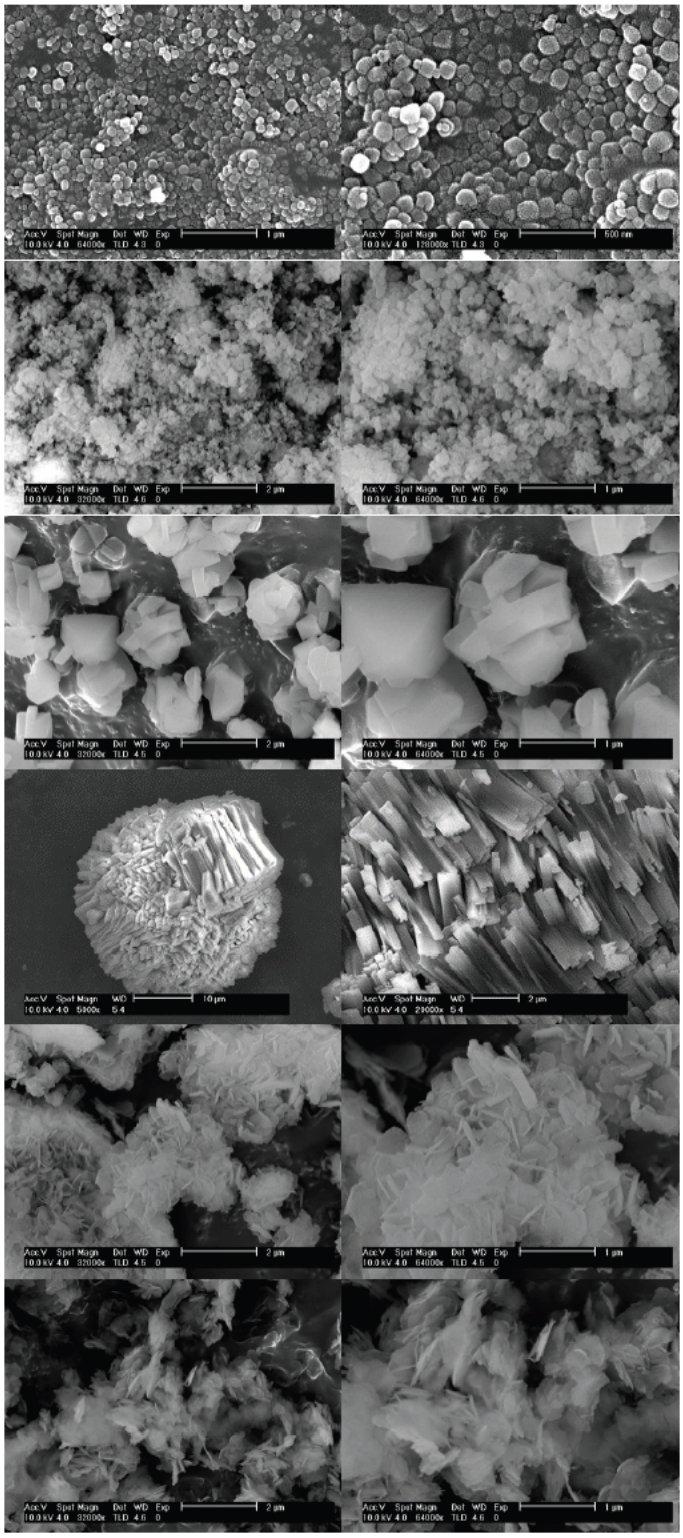

Fig. S2. SEM images of Cu/zeolites (From top to bottom: ZSM-5, Beta, Y, Mordenite, Ferrierite, and MCM-49). The different morphologies unique to the zeolites include Cu/ZSM-5 nanosphere

(~100 nm), Cu/Beta irregular nanoparticles (~120 nm), Cu/Y polyhedrons (~1300 nm), Cu/Mordenite bundled rods (~800 nm), Cu/Ferrierite nanosheets (~350 nm) and Cu/MCM-49 nanosheets (~250 nm).

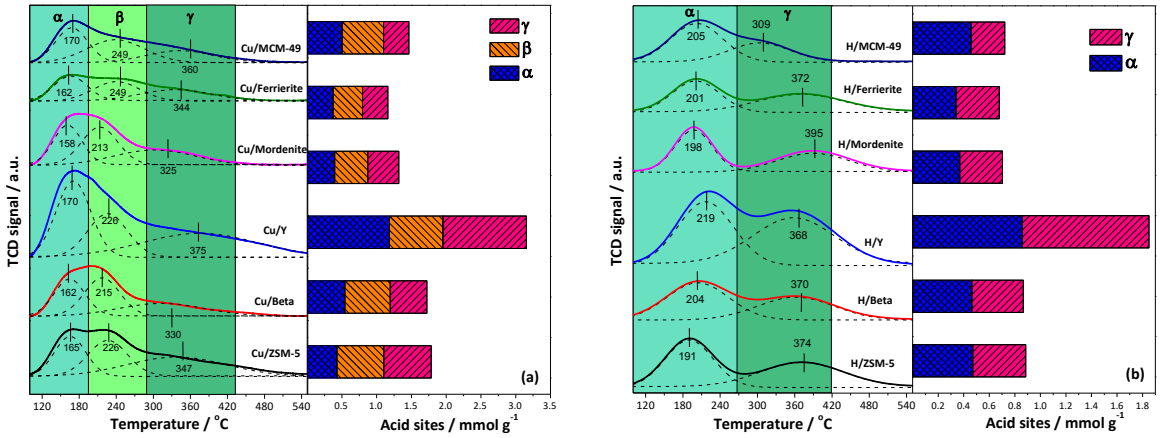

Fig. S3. NH_3-TPD profiles and acid sites quantification of (a) Cu/zeolites and (b) pristine H-zeolites.

The NH_3-TPD measurements were carried out to determine the amount and strength of acid sites on Cu/zeolites (Fig. S3).[S1,S2] Three NH_3 desorption peaks belonging to the weak (α, 120-200 °C), moderate (β, 200-290 °C), and strong (γ, 300-500 °C) acid sites could be measured.[S3] The Cu/Y has the highest amount of acid sites, followed by nano Cu/ZSM-5, Cu/Beta, Cu/MCM-49, Cu/Mordenite and Cu/Ferrierite. Besides the configurations of the framework Al, the amount of acid sites is partly accounted for by the specific surface area of the Cu/zeolites, such as that exemplified by the highest SSA Cu/Y. Interestingly, the amount of acid sites on Cu/zeolites was actually increased compared to the pristine zeolites (Fig. S3), particularly those of moderate acid strength that did not exist in the latter. While the Cu cation exchange sites took place on the Brønsted acid sites of the zeolite surface, the resultant surface Cu species gave rise to a range of other Lewis and Brønsted acid sites of various strengths, and where NH_3 chemisorbs.

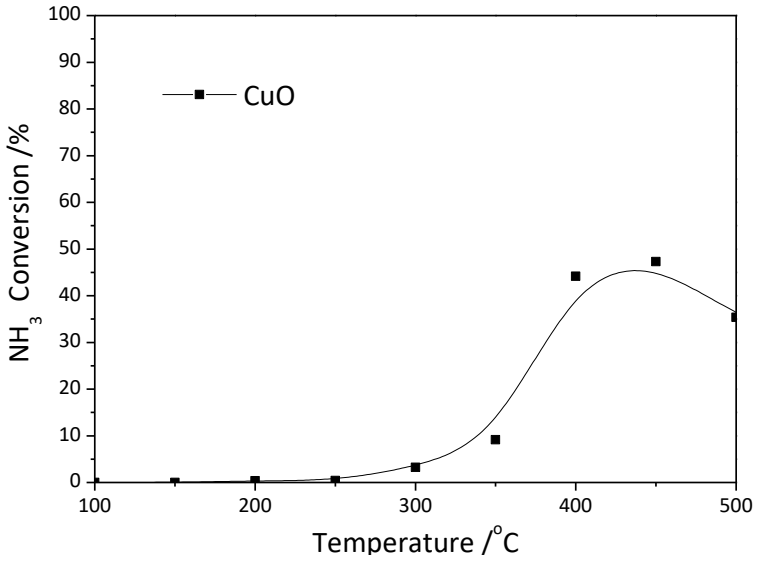

Fig. S4. The NH_3-SCO conversion on CuO.

Table S1. Comparison of different catalysts for selective catalytic oxidation of NH_3 to N_2

Catalyst		NH_3 Conversion / Temperature	Selectivity to N_2 / Temperature	Reaction conditions	Ref.
Noble metal	2.5 % Pd/Y	100 % / 250 °C	95 % / 250 °C	0.5% NH_3, 2.5% O_2, total flow 40 mL min^{-1}, catalyst: 0.1 g, GHSV: 19,200 h^{-1}	S4
	Mesoporous RuO_2	100 % / 250 °C	78 % / 250 °C	1000 ppm NH_3, 2% O_2, total flow 100 mL min^{-1}, catalyst: 0.08 g	S5
	10 % Ag/Al_2O_3	98 % / 100 °C	64 % / 100 °C	500 ppm NH_3, 10% O_2, total flow 300 mL min^{-1}, GHSV: 28000 h^{-1}	S6
	0.5 % Pt/ZSM-5	82 % / 200 °C	82 % / 200 °C	1000 ppm NH_3, 10% O_2, total flow 350 mL min^{-1}, catalyst: 0.2 g	This work
	0.5 % Ag/ZSM-5	93 % / 400 °C	73 % / 400 °C	1000 ppm NH_3, 10% O_2, total flow 350 mL min^{-1}, catalyst: 0.2 g	This work
	0.5 % Pd/ZSM-5	81 % / 200 °C	68 % / 200 °C	1000 ppm NH_3, 10% O_2, total flow 350 mL min^{-1}, catalyst: 0.2 g	This work
Transition metal	20 % CuO/Al_2O_3-ZrO_2	19 % / 200 °C	100 % / 200 °C	500 ppm NH_3, 5% O_2, total flow 200 mL min^{-1}, catalyst: 0.1 g	S7
	3% Fe/ZSM-5	82 % / 300 °C	82 % / 300 °C	1000 ppm NH_3, 10% O_2, total flow 350 mL min^{-1}, catalyst: 0.2 g	This work
	3 % Mn/ZSM-5	81 % / 300 °C	45 % / 300 °C	1000 ppm NH_3, 10% O_2, total flow 350 mL min^{-1}, catalyst: 0.2 g	This work
	4.08% Cu/SSZ-13	94 % / 200 °C	97 % / 200 °C	500 ppm NH_3, 5% O_2, total flow 200 mL min^{-1}, catalyst: 0.05 g, GHSV: 160,000 h^{-1}	S8
	6% Cu/SAPO-34	97 % / 250 °C	92 % / 250 °C	500 ppm NH_3, 21% O_2, total flow 1666 mL min^{-1}, GHSV: 250,000 h^{-1}	S9
	3% Cu/ZSM-5	98 % / 250 °C	98 % / 250 °C	1000 ppm NH_3, 10% O_2, total flow 350 mL min^{-1}, catalyst: 0.2 g	This work
	3% Cu/Beta	99 % / 300 °C	99 % / 300 °C	1000 ppm NH_3, 10% O_2, total flow 350 mL min^{-1}, catalyst: 0.2 g	This work
	3% Cu/Y	99 % / 350 °C	92 % / 350 °C	1000 ppm NH_3, 10% O_2, total flow 350 mL min^{-1}, catalyst: 0.2 g	This work
	3% Cu/Mordenite	100 % / 350 °C	92 % / 350 °C	1000 ppm NH_3, 10% O_2, total flow 350 mL min^{-1}, catalyst: 0.2 g	This work
	3% Cu/Ferrierite	100 % / 400 °C	100 % / 400 °C	1000 ppm NH_3, 10% O_2, total flow 350 mL min^{-1}, catalyst: 0.2 g	This work
	3% Cu/MCM-49	96 % / 350 °C	92 % / 350 °C	1000 ppm NH_3, 10% O_2, total flow 350 mL min^{-1}, catalyst: 0.2 g	This work

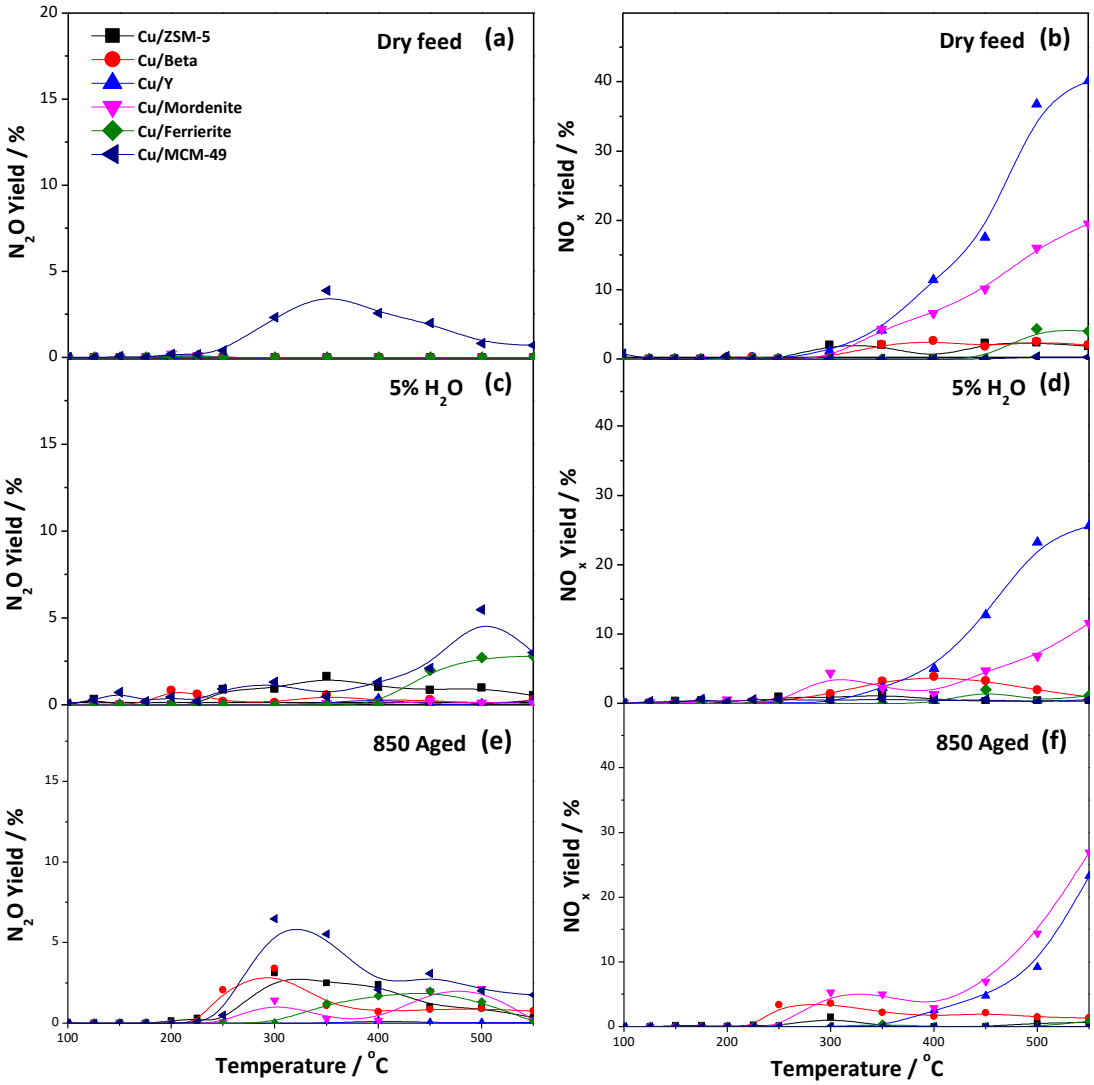

Fig. S5. Byproducts of N_2O and NO_x yields on different Cu/zeolites during the NH_3-SCO under (a, b) dry feed and (c, d) the addition of 5% H_2O in the feed gas, as well as that (c, d) after hydrothermal treatment (e, f). Conditions: 1000 ppm NH_3, 10% O_2, GHSV = 45,000 h^{-1}.

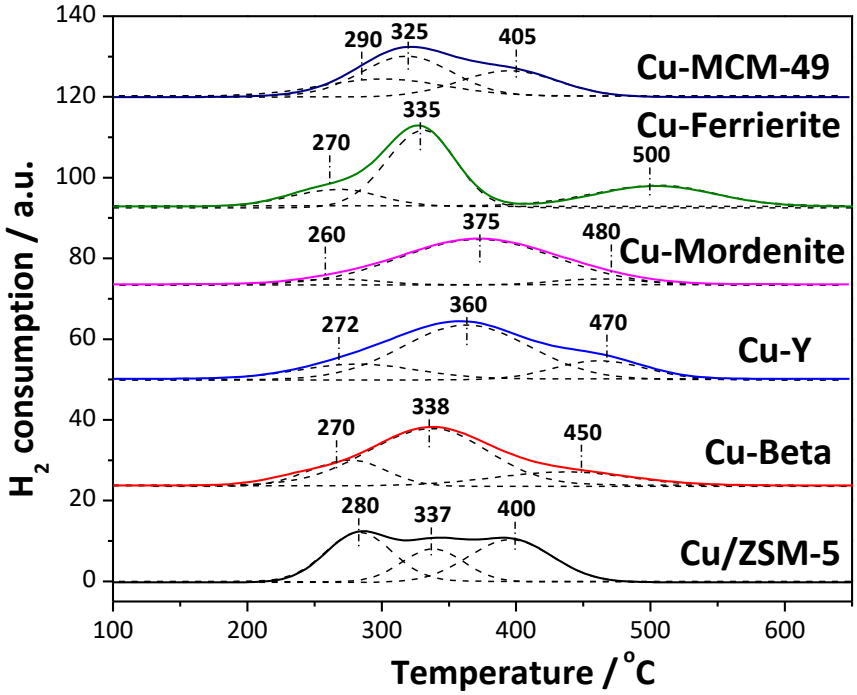

Fig. S6. H_2-TPR profiles of hydrothermally aged Cu/zeolites (zeolites: ZSM-5, Beta, Y, Mordenite, Ferrierite, MCM-49).

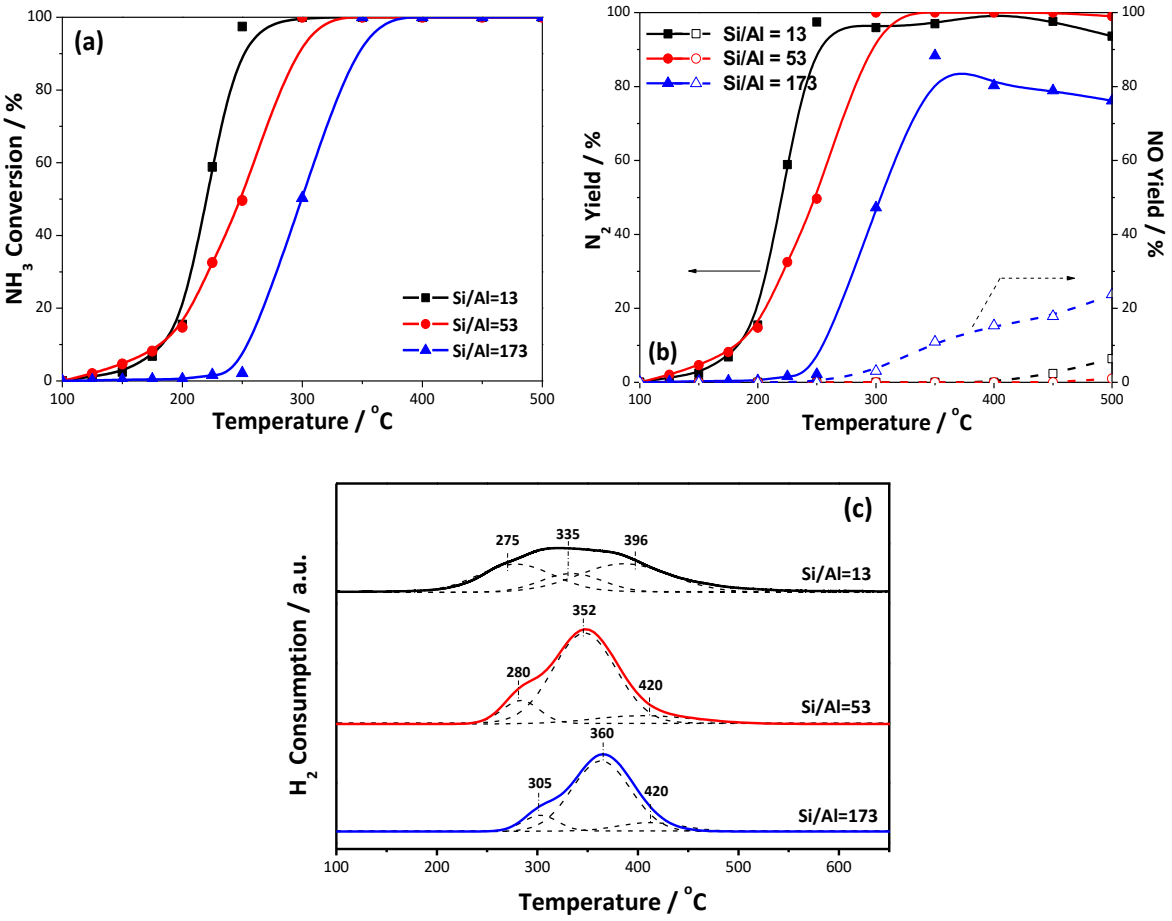

Fig. S7. (a) NH_3 conversion and (b) the corresponding products yield of Cu/ZSM-5 with different Si/Al ratios, i.e., 13, 53 and 173 in NH_3-SCO reaction. Conditions: 1000 ppm NH_3, 10% O_2, GHSV = 45,000 h^{-1}. Shown in (c) is the H_2-TPR profiles of Cu/ZSM-5 (Si/Al = 13, 53 and 173).

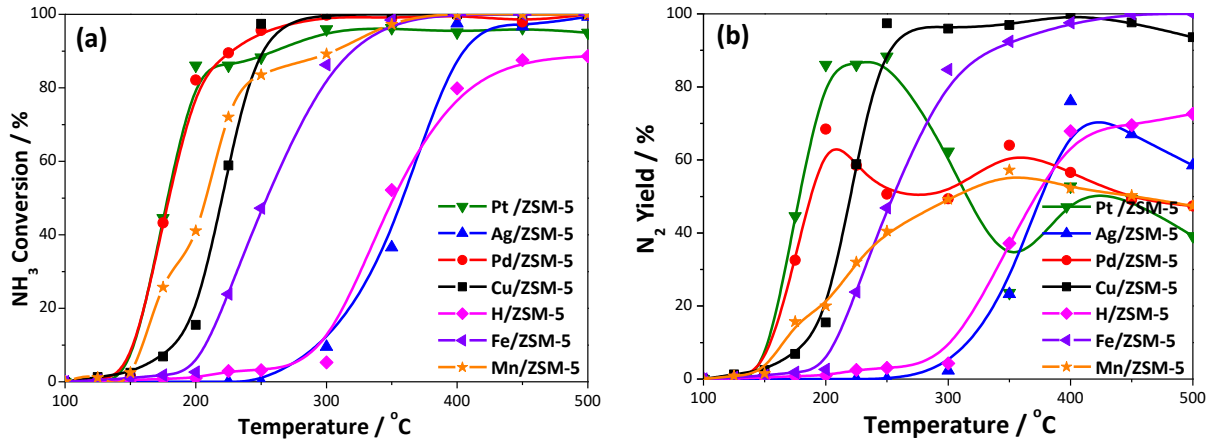

Fig. S8. (a) NH_3 conversion and (b) the corresponding products yield of different metal (Pt, Ag, Pd, Cu, Fe, Mn)/ZSM-5 as well as H/ZSM-5 in NH_3-SCO reaction. Conditions: 1000 ppm NH_3, 10% O_2, GHSV = 45,000 h^{-1}.

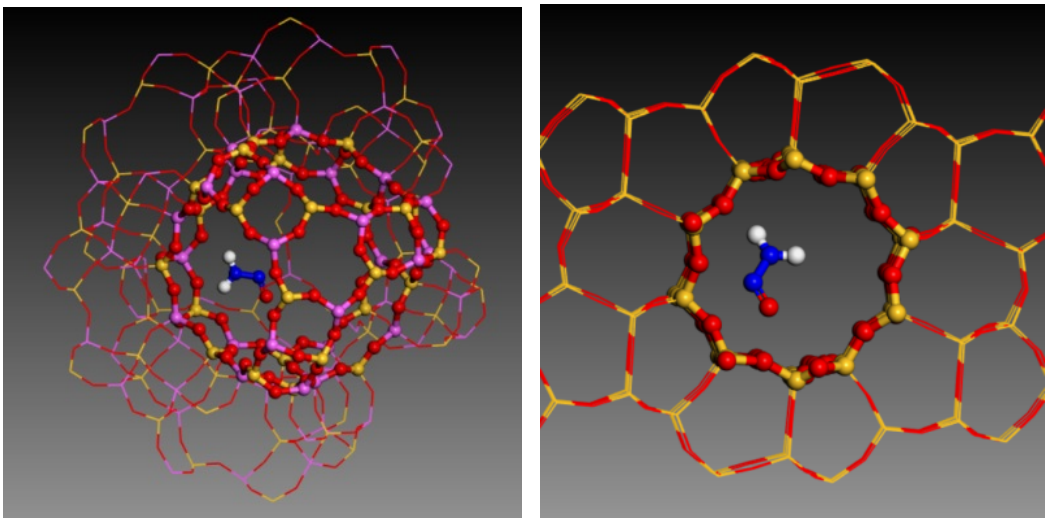

Fig. S9. Comparison of the size of the NH_2NO intermediate molecule with respect to the supercage of Y-zeolite (left) and the 10-MR pore channel of ZSM-5 (right).

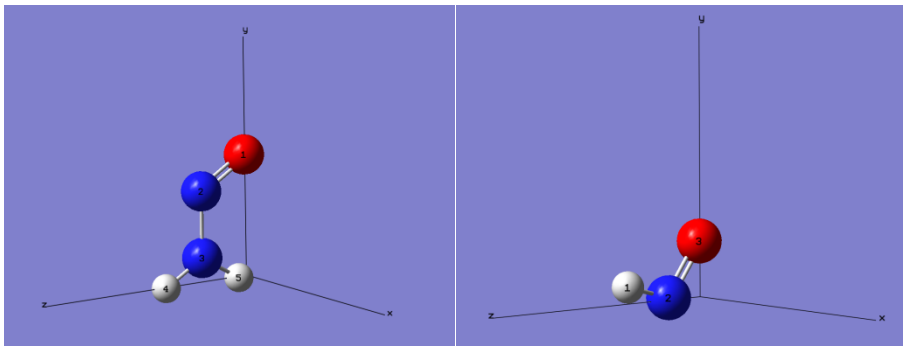

The coordinates of atoms in the model of H_2NNO

Tag	Symbol	X	Y	Z
1	O	-0.0009467	2.5331818	0.0190213
2	N	-0.0061983	1.8998243	1.0938508
3	N	-0.006037	0.5003933	1.089249
4	H	-0.0109647	-0.0212557	1.9929278
5	H	0.0004643	-0.0282503	0.188506

The coordinates of atoms in the model of HNO

Tag	Symbol	X	Y	Z
1	H	0.025934	0.314191	1.761022
2	N	0.009699	0.043334	0.767888
3	O	0.019284	1.034615	0.032851

Fig. S10. Construction of the HNO and NH_2NO intermediate molecules, and the respective atomic coordinates

References

S1 C. Niu, X. Shi, F. Liu, K. Liu, L. Xie, Y. You, H. He, High hydrothermal stability of Cu-SAPO-34 catalysts for the NH_3-SCR of NO_x, *Chem. Eng. J.*, 2016, **294,** 254–263.

S2 W. Wan, T. Fu, R. Qi, J. Shao, Zhong Li, Coeffect of Na^+ and tetrapropylammonium (TPA^+) in alkali treatment on the fabrication of mesoporous ZSM-5 catalyst for methanol-to-hydrocarbons reactions, *Ind. Eng. Chem. Res.*, 2016, **55,** 13040–13049.

S3 H. Wang, R. Xu, Y. Jin, R. Zhang, Zeolite structure effects on Cu active center, SCR performance and stability of Cu-zeolite catalysts, *Catal. Today*, 2019, **327,** 295–307.

S4 M. Jablonska, A. Krol, E. Kukulska-Zajac, K. Tarach, L. Chmielarz, K. Gora-Marek, Zeolite Y modified with palladium as effective catalyst for selective catalytic oxidation of ammonia to nitrogen, *J. Catal.* 2014, **316,** 36−46.

S5 X. Cui, J. Zhou, Z. Ye, H. Chen, L. Li, M. Ruan, J. Shi, Selective catalytic oxidation of ammonia to nitrogen over mesoporous CuO/RuO_2 synthesized by co-nanocasting-replication method, *J. Catal.* 2010, **270,** 310−317.

S6 F. Wang, J. Ma, G. He, M. Chen, C. Zhang, H. He, Nanosize effect of Al_2O_3 in Ag/Al_2O_3 catalyst for the selective catalytic oxidation of ammonia, *ACS Catal.* 2018, **8,** 2670−2682.

S7 X. Cui, L. Chen, Y. Wang, H. Chen, W. Zhao, Y. Li, J. Shi, Fabrication of hierarchically porous RuO_2-CuO/Al-ZrO_2 composite as highly efficient catalyst for ammonia-selective catalytic oxidation, *ACS Catal.* 2014, **4,** 2195−2206.

S8 T. Zhang, H. Chang, Y. You, C. Shi, J. Li, Excellent activity and selectivity of one-pot synthesized Cu-SSZ-13 catalyst in the selective catalytic oxidation of ammonia to nitrogen, *Environ. Sci. Technol.*, 2018, **52,** 4802−4808.

S9 F. Han, M. Yuan, S. Mine, H. Sun, H. Chen, T. Toyao, M. Matsuoka, K. Zhu, J. Zhang, W. Wang, T. Xue, Formation of highly active superoxide sites on CuO nanoclusters encapsulated in SAPO-34 for catalytic selective ammonia oxidation, *ACS Catal.* 2019, **9,** 10398−10408.